*Proc. Natl. Acad. Sci. USA*
Vol. 87, pp. 9833–9837, December 1990
Neurobiology

# Specificity of cell–cell coupling in rat optic nerve astrocytes *in vitro*

(gap junction/patch clamp/Lucifer yellow)

H. SONTHEIMER*, J. E. MINTURN, J. A. BLACK, S. G. WAXMAN, AND B. R. RANSOM

Department of Neurology, Yale University School of Medicine, New Haven, CT 06510; and Eastern Paralyzed Veterans Association Neuroscience Research Center, Veterans Administration Medical Center, West Haven, CT 06516

*Communicated by Pasko Rakic, September 24, 1990*

**ABSTRACT** **Intercellular coupling was studied in cultured rat optic nerve astrocytes individually characterized by A2B5 antibody staining. The presence of cell coupling was assessed by injecting single cells with the low molecular weight fluorescent dye Lucifer yellow and noting dye passage into adjacent cells; cell coupling was also studied by analyzing the decay phase of current transients recorded in response to small voltage steps using whole-cell patch-clamp recording. Cell coupling was restricted to A2B5$^-$ astrocytes, the majority of which had a flat fibroblast-like appearance and was never observed in A2B5$^+$ stellate-shaped astrocytes. Furthermore, A2B5$^-$ astrocytes showed coupling only to A2B5$^-$ and never to A2B5$^+$ astrocytes. Analysis of current transients provided an additional indicator for cell coupling. Astrocytes that showed dye coupling to at least one neighboring cell required the sum of two exponential functions to fit current transients, whereas a single exponential function sufficed to fit transients in cells that were not dye coupled. The specificity of cell coupling in cultured rat optic nerve astrocytes suggests that predominantly A2B5$^-$ astrocytes comprise a coupled glial syncytium; this physiological feature of these cells may be a specialized adaptation for "spatial buffering," the transport of K$^+$ away from areas of focal extracellular accumulation. On the other hand, A2B5$^+$ astrocytes form an uncoupled subpopulation of rat optic nerve glial cells that may serve different functions.**

Astrocytes form gap junctions with adjacent astrocytes (1) and these large intercellular channels are believed to link the cells into a three-dimensional network. As previously shown for a variety of cell systems, these connections allow direct cytoplasmic diffusion of inorganic and small organic molecules between cells (2). Injection of the low molecular weight fluorescent dye Lucifer yellow (LY) (3) into single astrocytes has revealed dye spread into adjacent astrocytes, thereby indicating gap junctional communication, in cortical slices (4), spinal cord (5), cortical (6) and cerebellar cell cultures (7), and rat optic nerve (RON) *in situ* (8). Similarly, coupling of cultured astrocytes was apparent in studies in which laser photobleaching techniques were used (9).

Cultures from RON provide a well-described glial cell system in which two types of astrocytes can be distinguished morphologically and by their ability to bind the monoclonal antibody A2B5 (reviewed in ref. 10). *In vitro* A2B5$^-$/GFAP$^+$ (glial fibrillary acidic protein) astrocytes [termed type 1 astrocytes, (11)] have a fibroblast-like appearance and are believed to develop from a specific, still poorly characterized, progenitor cell. In contrast, A2B5$^+$/GFAP$^+$ astrocytes [termed type 2 astrocytes (11)] have a stellate appearance and share a common precursor cell, the O2A progenitor cell, with oligodendrocytes (10, 11). Further differences between these types of astrocytes have become apparent and include, but are not limited to, their response to and the secretion of growth factors, their antigen profile (10), and their pattern of ion channel expression (12, 13). A similar classification of astrocytes based on binding of A2B5 antibody has been described for cerebellar cultures (14). Not all areas of the brain yield astrocytes that can be subdivided in this manner; astrocytes in cultures from hippocampus, for example, do not bind A2B5 (15). The present study addresses the question of whether the two well-delineated classes of astrocytes in RON are functionally coupled to one another.

## METHODS

**Cell Cultures.** Astrocyte cultures were obtained from postnatal day 7 Wistar RONs. Optic nerves (excluding the chiasm) were incubated for 45 min at 37°C in an enzyme solution containing Earle's salts, papain (30 units/ml), 1.5 mM $CaCl_2$, 0.5 mM EDTA, and 1.65 mM L-cysteine. After trituration, the cell suspensions were plated onto collagen/poly-D-lysine-coated coverslips (100,000 cells per ml). Cultures were maintained in Earle's minimum essential medium containing 5% fetal bovine serum with serum extender (Collaborative Research), penicillin/streptomycin (500 units/ml), and 20 mM glucose, at 37°C in a 5% $CO_2$/95% air atmosphere. Staining with anti-GFAP antibody demonstrated that the cell population in these cultures consisted almost exclusively of astrocytes (>98%).

**Dye Injection and Cell Identification.** Experiments were carried out on the stage of an inverted microscope equipped with Hofmann interference contrast and epifluorescence optics. Dye-filled cells could be viewed on-line via either eyepieces or a low illumination video camera (Dage-MTI, Michigan City, IN) attached to the microscope. Cultures were continuously superfused with a solution containing 130 mM NaCl, 1.2 mM $MgSO_4$, 1.0 mM $CaCl_2$, 1.6 mM $Na_2HPO_4$, 0.4 mM $NaH_2PO_4$, 10.5 mM glucose, 32.5 mM Hepes (acid). The pH was adjusted to 7.4 with NaOH.

Astrocytes were initially selected by morphological criteria. We assumed that stellate appearing cells would be A2B5$^+$ astrocytes and that flat, fibroblast-like cells would be A2B5$^-$ astrocytes. To definitively classify these cells, we stained them by using antibody to the surface glycoprotein A2B5. After successful dye injections, cells were fixed on ice in 4% paraformaldehyde for 5 min and underwent reaction with A2B5 antibody (an IgM; American Type Culture Collection). In almost all instances, initial morphological identification was confirmed by immunostaining. However, in the case of discrepancy, priority was given to identification by antibody staining.

Cell–cell coupling was assayed by examining the spread of the fluorescent dye LY (3) after it was injected into single astrocytes. Current recordings were obtained from all injected cells. Current recordings and dye injections were

The publication costs of this article were defrayed in part by page charge payment. This article must therefore be hereby marked "*advertisement*" in accordance with 18 U.S.C. §1734 solely to indicate this fact.

Abbreviations: DIV, days *in vitro*; GFAP, glial fibrillary acidic protein; LY, Lucifer yellow; RON, rat optic nerve.

*To whom reprint requests should be addressed at: Department of Neurology LCI 712, Yale University, School of Medicine, 333 Cedar Street, New Haven, CT 06510.

obtained by the whole-cell mode of the patch-clamp technique (16). The patch pipette solution was supplemented with 0.2% LY (dilithium salt; Sigma). The pipette solution contained 120 mM *N*-methyl-D-glucamine, 20 mM tetraethylammonium chloride, 1 mM $MgCl_2$, 0.2 mM $CaCl_2$, 10 mM EGTA, 10 mM Hepes (sodium salt). The pH was adjusted to 7.4 with HCl. Patch-clamp electrodes filled with this pipette solution yielded resistances between 3 and 5 MΩ.

After achieving a whole-cell recording, LY filled the recorded cell almost instantaneously. To facilitate dye spread into adjacent cells, the recording mode was switched to current clamp and a train of negative current steps (500 pA; 50 Hz) was applied for 3 min; this improved dye spread due to the anionic nature of LY.

Dye coupling between the recorded cells and adjacent cells was evaluated by examination of fluorescence photomicrographs of the field under observation. Dye-filled cells were evaluated for coupling only if they were surrounded by numerous cells.

**Electrophysiology and Evaluation of Capacity Transients.** Voltage-clamp recordings were obtained by the whole-cell mode of the patch-clamp technique (16). An Axopatch 1D amplifier (Axon Instruments) was used and electrodes (TW150F-4; WP Instruments, Waltham, MA) were Sylgard-coated (Dow/Corning) and filled with the solution described above. Whole-cell currents were recorded in response to brief (10–30 msec) voltage steps (5 mV). Electrode capacitance was canceled through the amplifier's cancelation cir-

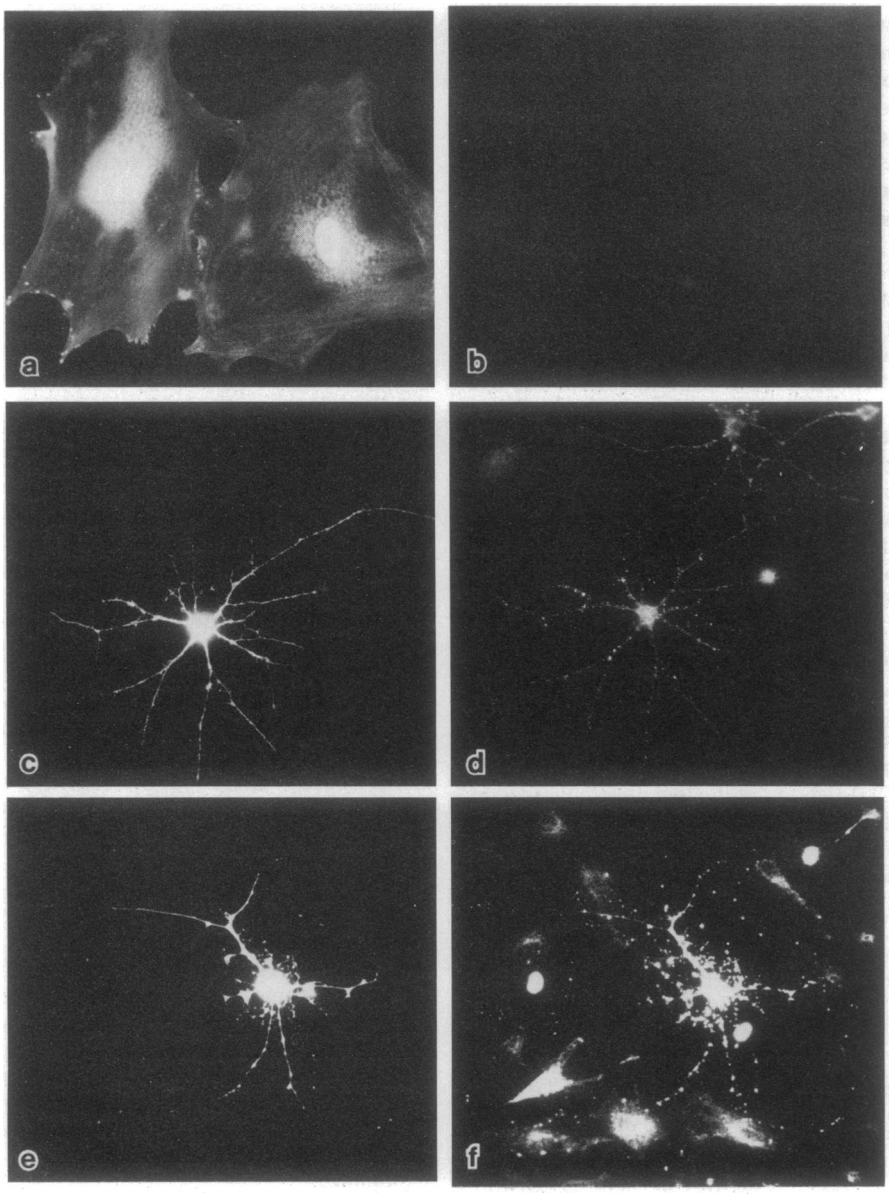


FIG. 1. Dye injections into RON astrocytes. LY was injected into two morphologically distinct types of astrocytes with either stellate (*c* and *e*) or flat fibroblast-like (*a*) appearance. Only in fibroblast-like astrocytes was dye spread into adjacent cells observed (*a*). In stellate astrocytes, the dye remained exclusively in the injected cell (*c* and *e*). Cells were identified according to their expression of A2B5 antigen. After immunostaining for A2B5, fluorescent photomicrographs (*b*, *d*, and *f*) show the same microscopic field illustrated in *a*, *c*, and *e*. These revealed that the fibroblast-like cells were $A2B5^-$ astrocytes, whereas the stellate-appearing cells were $A2B5^+$ astrocytes. (*a* and *b*) Two adjacent $A2B5^-$ astrocytes. The injected $A2B5^-$ astrocyte showed dye coupling to an adjacent $A2B5^-$ astrocyte. (*c* and *d*) Three adjacent $A2B5^+$ astrocytes. The injected $A2B5^+$ astrocyte did not exhibit dye coupling to any other cells. (*e* and *f*) An $A2B5^+$ cell on a cluster of $A2B5^-$ astrocytes. When the $A2B5^+$ astrocyte was injected with LY, no dye spread was observed into the bed layer of $A2B5^-$ astrocytes. Note that staining with A2B5 antibody often showed less intense, unspecific, or background staining of flat fibroblast-like astrocytes as shown here. This example was intentionally chosen so that the bed layer of astrocytes could be seen, to illustrate the absence of coupling to the LY-filled $A2B5^+$ cell.

cuitry after a gigohm seal was established in the cell-attached configuration. Current recording and stimulation were achieved by using an analog/digital–digital/analog converter interfaced with an IBM compatible computer (Dell 310). Data acquisition and analysis were controlled by custom programmed software. Data were typically sampled at 25-$\mu$sec intervals.

Current transients were fitted to an exponential function of the form:

$$Y(t) = a + b \times \exp[-c/t] + d \times \exp[-e/t],$$

using an algorithm to minimize the least-squares error.

Transients could be well fitted by either single or double exponential functions, although in some instances higher-degree exponential functions may have yielded slightly better fits.

## RESULTS

To study coupling among the two types of astrocytes derived from optic nerve, we obtained whole-cell recordings with LY-containing patch pipettes. Cells were only studied by patch clamp if they were surrounded by numerous cells and appeared to touch two or more neighboring cells as judged by the phase-contrast image. Astrocytes cultured for 1–2 days *in vitro* (DIV) grew in small groups of 3–10 cells each, scattered over the coverslip. After 7–10 DIV most of the coverslip was overgrown by a monolayer of predominantly flat fibroblast-like A2B5$^-$ astrocytes. A2B5$^+$ cells grew either on this layer of A2B5$^-$ astrocytes or at the edges, where A2B5$^-$ cells were sparse. Astrocytes from cultures ranging in age from 1 to 20 DIV were studied.

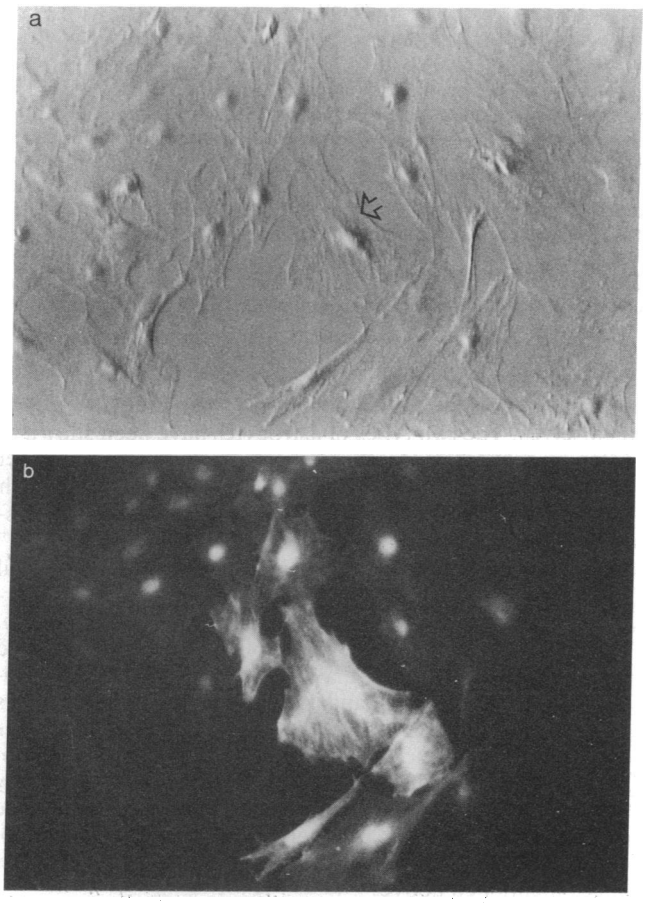


FIG. 2. Dye coupling in astrocytes after exposure to octanol. Coverslips with astrocytes were exposed to 200 nM octanol for at least 10 min before single cells were injected with LY. Dye spread among A2B5$^-$ astrocytes was still observed after octanol exposure and could be as pronounced as shown in *b*. Virtually all cells visible in the field (*a*) were dye coupled to the cell injected (*b*). The cell injected is marked with an arrowhead in *a*.

Fig. 1 shows typical examples of dye-injected cells in several configurations; i.e., groups of adjacent A2B5$^-$ astrocytes (Fig. 1 *a* and *b*), groups of adjacent A2B5$^+$ astrocytes (Fig. 1 *c* and *d*) and clusters of both A2B5$^-$ and A2B5$^+$ astrocytes (Fig. 1 *e* and *f*). As exemplified in Fig. 1, there was often coupling between A2B5$^-$ astrocytes (Fig. 1 *a* and *b*). In contrast, A2B5$^+$ astrocytes were not dye coupled to other A2B5$^+$ astrocytes (Fig. 1 *c* and *d*) or to A2B5$^-$ astrocytes (Fig. 1 *e* and *f*). Since A2B5$^+$ cells may grow on a layer of A2B5$^-$ astrocytes, large areas of cell membrane are juxtaposed. However, examining regions where single A2B5$^+$ astrocytes grew on a bed layer of A2B5$^-$ astrocytes did not reveal dye spread between A2B5$^+$ and A2B5$^-$ astrocytes when LY was injected into A2B5$^+$ astrocytes (Fig. 1 *e* and *f*; see Fig. 4*c Top*) or into one of the A2B5$^-$ astrocytes forming the substrate (data not shown).

In most instances of coupling, the dye spread into two to five neighboring cells but occasionally included all cells visible in the field (>30 cells; e.g., Fig. 2). Strong coupling among A2B5$^-$ astrocytes could still be observed after cultures were exposed to octanol (200 nM; 10 min prior to dye injection; $n = 6$), which has been shown to inhibit cell coupling in isolated rat liver cells (17) and murine pancreatic acinar cells (18), and abolished dye-coupling in cultured rat hippocampal astrocytes (19).

Dye spread between A2B5$^-$ astrocytes was frequently observed at all ages studied ($n = 30$ of 65; 1–20 DIV). The histogram in Fig. 3 represents pooled data from the following age groups: 1–6, 7–12, and 13–20 DIV. The percentage of A2B5$^-$ dye-coupled astrocytes increased with time in culture from 24% between 1 and 6 DIV, to 73% after 13–20 DIV (Fig. 3). In contrast, dye spread was never observed between adjacent A2B5$^+$ astrocytes regardless of time in culture ($n = 58$; Fig. 3).

In addition to the intercellular spread of LY, we analyzed current transients in response to brief de- or hyperpolarizing voltage steps in voltage-clamped astrocytes. In an ideal, isolated, spherical cell, such current transients should decay with a time constant proportional to the membrane capacitance ($t = R \times C$). Despite the nonspherical nature of the astrocytes studied here, such transients could be fitted reasonably well by single exponential functions with time con-

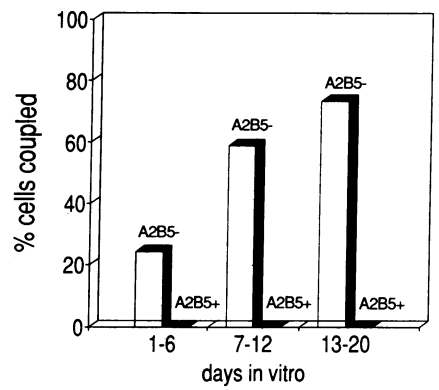


FIG. 3. Time course of dye coupling in A2B5$^-$ and A2B5$^+$ astrocytes. The percentage of astrocytes of both antigenic phenotypes was plotted as a function of time in culture. Cells from three time groups were pooled: 1–6 (A2B5$^-$, $n = 33$; A2B5$^+$, $n = 26$), 7–12 (A2B5$^-$, $n = 17$; A2B5$^+$, $n = 22$), and 13–20 (A2B5$^-$, $n = 15$; A2B5$^+$, $n = 10$) DIV. The percentage of A2B5$^-$ astrocytes exhibiting dye coupling increased with time in culture from 24% between days 1 and 6 to 73% after 13–20 DIV. In contrast, A2B5$^+$ astrocytes did not exhibit dye coupling at any time in culture up to 20 DIV.

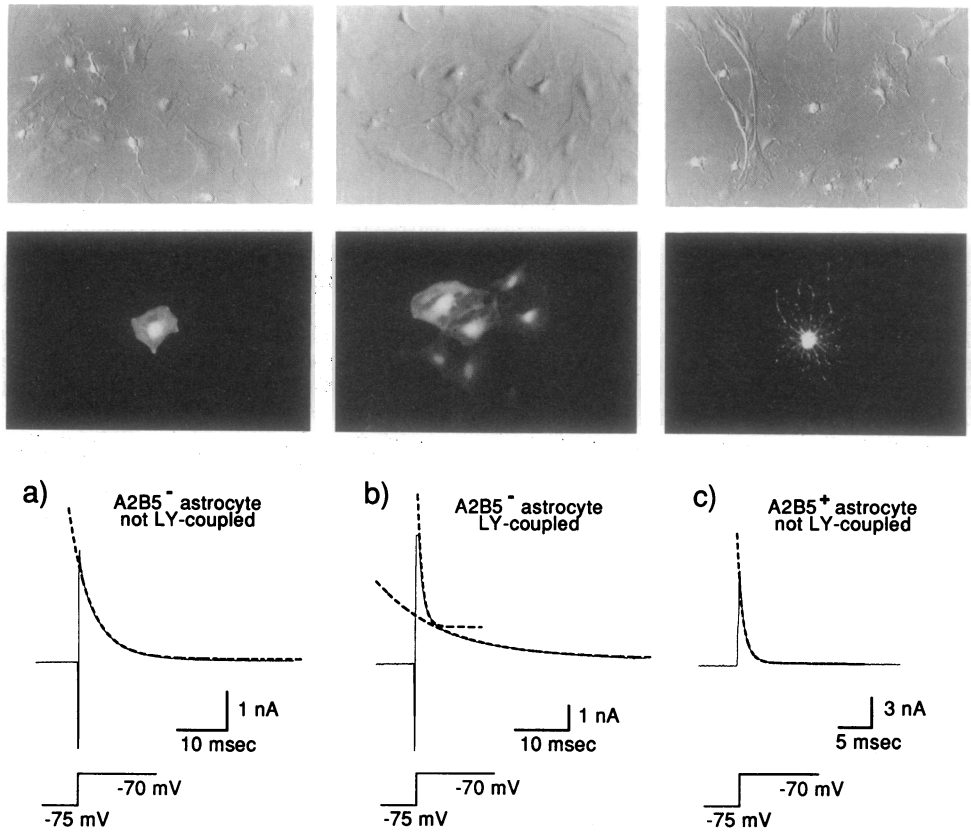


FIG. 4. Analysis of current transients in astrocytes in relationship to the presence or absence of dye coupling. Current transients in response to small depolarizing voltage steps of 5 mV were fitted to single or double exponential functions. In cells that did not show dye coupling, the transients could be fitted reasonably well by a single exponential function (time constant, 0.5–5 msec). The record displayed in *a* was obtained from a physically isolated A2B5⁻ astrocyte after 6 DIV. Phase-contrast and fluorescent photomicrographs of the recorded cell are shown above each recording. The time constant for the cell in *a* was 4.8 msec. In astrocytes that showed dye spread into adjacent cells, the current transients were best fit by the sum of two exponentials with time constants of 0.5–3 and 5–15 msec, respectively. The record displayed in *b* was obtained from an A2B5⁻ astrocyte after 6 DIV that was dye coupled to six adjacent A2B5⁻ astrocytes (see photomicrographs). The current decay was best fit by the sum of two exponentials with time constants of 0.9 and 12 msec, respectively. The two functions were imposed on the original current trace and displayed separately. (*c*) Current transient recorded in A2B5⁺ astrocyte after 10 DIV that was not LY coupled to neighboring cells. As shown in *a* for an isolated A2B5⁻ astrocyte, the current transient could be best fit by a single exponential function with a time constant of ≈1.6 msec.

stants proportional to cell membrane capacitance when recordings were obtained in isolated astrocytes. An example of such a recording obtained from an isolated A2B5⁻ astrocyte is displayed in Fig. 4*a*. Phase-contrast and fluorescence photomicrographs show the appearance of the cell studied (Fig. 4). Cells that exhibited dye spread into at least one adjacent cell exhibited current transients that deviated from a single exponential function and required the sum of two or more exponentials for an adequate fit (Fig. 4*b*). We limited our fitting analysis to the sum of two exponentials, since time constants of possible third exponentials were close to the slower of the two. In all instances in which we observed dye spread into neighboring cells ($n$ = 30), analysis of the current transient revealed a clear multiexponential current decay. The two time constants fitted to our data typically differed by 0.5–1 order of magnitude and were between 0.5 and 3 msec for the fast, and 5–15 msec for the slow exponential. In all astrocytes that lacked dye coupling, or astrocytes that were physically isolated, current transients decayed with a single, comparatively faster (0.5–5 msec) time constant; this applied to all A2B5⁻ astrocytes that lacked dye coupling ($n$ = 35; Fig. 4*a*) and was always the case in A2B5⁺ astrocytes ($n$ = 58; Fig. 4*c*).

## DISCUSSION

The two types of astrocytes that are characteristic of cultures from RON—i.e., A2B5⁻ and A2B5⁺ astrocytes—differed absolutely with regard to dye coupling. The A2B5⁻ astrocytes showed coupling to each other, but never to A2B5⁺ astrocytes, nor did A2B5⁺ astrocytes show coupling among themselves. The two types of astrocytes have been shown to differ in a number of other aspects including ion-channel patterns (12, 13, 20) and response to and release of growth factors (10). Electrophysiologically, the two types are distinct with regard to $Na^+$-current expression, with A2B5⁺ astrocytes expressing currents that are similar to neuronal $Na^+$ currents and A2B5⁻ astrocytes expressing a $Na^+$ current with a more hyperpolarized inactivation curve (20, 21). The presence of intercellular coupling allows the coupled population of cells to share a common intracellular environment in terms of ions and numerous organic molecules including second messengers and small hormones (2). This common cytoplasmic environment probably serves to promote homogenous physiological behavior; this is certainly the case for electrophysiological behavior. Thus, the absence of discernible coupling between A2B5⁻ and A2B5⁺ astrocytes may be critical for maintenance of some of the differences mentioned above.

Two methods have been used to assess cell coupling—the spread of LY into neighboring cells and the examination of current transient decays. Due to the size of LY molecules ($M_r$ 457.3) and its dilution in the cell cytoplasm, the capability of dye coupling to reveal small degrees of coupling is questionable. The use of two or more electrodes allows direct measurement of current spread among cells. At present,

however, few data are available allowing a quantitative comparison of dye coupling and electrical coupling. In *Heliosoma* neurons, strong electrical coupling—e.g., a coupling ratio of 0.5—was required to visualize LY spread across gap junctions (22). This value, however, appears high and may relate to the morphology of *Heliosoma* neurons in which long cellular processes and relatively large cytoplasmic components may substantially hinder diffusion. Current injected into amphibian Müller cells, astrocyte-like cells in the retina, is attenuated >50-fold in adjacent cells 50 $\mu$m away (23). Given that LY spread was visible at distances up to 130 $\mu$m from the point of injection, involving spread across four sequential Müller cells, dye spread would have still been visible at a coupling ratio of <0.02 (23). Double electrode experiments would provide a direct comparison of dye and electrical coupling in astrocytes and substantiate the sensitivity of LY spread for the detection of astrocyte coupling. Preliminary double electrode patch-clamp studies suggest a high sensitivity of LY spread, since clear dye coupling was still visible between cell pairs exhibiting a coupling ratio of only 0.1. It is possible that A2B5$^+$ astrocytes show weak coupling (i.e., coupling ratio <0.1) that cannot be revealed by dye spread; weak electrical coupling in the absence of dye coupling has been shown between some oligodendrocytes (5) and between astrocytes and oligodendrocytes in cultured mouse spinal cord (24). It was suggested that such weak coupling could subserve metabolic interactions between these cells rather than allowing strong electrical interactions.

The congruency of dye coupling and multiexponential current transient decay suggests that current transients provide an electrical correlate to dye coupling. Therefore, their analysis may serve as an additional sensitive tool to assess cell coupling. A similar correlation was observed in a study of hippocampal astrocytes (19). Here the slower time constant could clearly be related to cell coupling, since it disappeared upon exposure to 100 nM octanol, which is known to inhibit cell coupling (17, 18) and eliminated dye coupling in the hippocampal astrocytes under study (19). One would expect, however, the junctional time constant to be smaller than the nonjunctional time constant, since both junctional resistance and capacitance are smaller (25). Thus, the biophysical explanation for the slower time constant associated with the presence of coupling remains to be clarified but it appears that the ability to discern the slower time constant is related to the specific solution used and its diffusion into neighboring cells.

In RON astrocytes, exposure to octanol failed to uncouple dye-coupled cell pairs ($n = 6$), suggesting that their junctional conductance may be regulated differently than in other cell types. It has been shown for a variety of cell types that junctional conductance is modulated in a complex way by intracellular [$Ca^{2+}$], intracellular [pH]$_i$, and second messengers (for reviews, see refs. 2 and 26).

One of the main functions proposed for astrocytes in the brain, "spatial buffering," the redistribution of focal increases in $K^+$ within the extracellular space (27), is believed to involve strong coupling among these cells to overcome extracellular diffusion limitations (28). In Müller cells in the axolotl retina, differential distribution of $K^+$ channels, with high density in the endfeet, leads to a "siphoning" of $K^+$ ions into the cells and away from areas with high $K^+$ concentration (29). As with A2B5$^-$ astrocytes in this study, Müller cells are coupled through gap junctions (30); it has previously been shown that coupling increases the spatial buffer capacity of Müller cells by 60% (23). Since it appears that only A2B5$^-$ astrocytes exhibit such pathways, A2B5$^+$ astrocytes would be less likely to participate in spatial buffering in the optic nerve, which may be a function exclusive to A2B5$^-$ astrocytes in this structure.

The absence of dye coupling between A2B5$^+$ astrocytes was surprising. It has been suggested that A2B5$^+$ astrocytes give rise to perinodal processes (31), and gap junctions have been observed on perinodal astrocytes *in situ* in the optic nerve (32). However, in those cases in which both cells contributing to the gap junction could be identified, gap junctions were located between perinodal astrocytes and oligodendrocytes (32). Astrocyte–oligodendrocyte coupling—as has been demonstrated electrophysiologically (24)—and/or the presence of gap junctions at a density too low to permit dye coupling would be consistent with the present results.

Because A2B5$^+$ astrocytes fail to make intercellular connections with other astrocytes, they form a uniquely isolated subset of cells. Unlike A2B5$^-$ astrocytes, they appear designed to function much more independently of one another. The purpose of this adaptation is presently not understood and must be a focus of future research, which must also seek to confirm that such a subpopulation of astrocytes exists in the RON *in vitro*.

This work was supported in part by grants from the National Institutes of Health; the National Multiple Sclerosis Society; and by the Medical Research Service, Department of Veterans Affairs. H.S. was supported by a Spinal Cord Research Fellowship from the Eastern Paralyzed Veterans Association; J.E.M. was supported in part by the American Heart Association.

1. Mugnaini, E. (1986) in *Astrocytes*, eds. Fedoroff, S. & Vernakis, A. (Academic, Orlando, FL), pp. 329–371.
2. Loewenstein, W. R. (1981) *Physiol. Rev.* **61**, 829–913.
3. Stewart, W. W. (1978) *Cell* **14**, 741–759.
4. Gutnick, M. J., Connors, B. W. & Ransom, B. R. (1981) *Brain Res.* **213**, 486–492.
5. Kettenmann, H., Orkand, R. K. & Schachner, M. (1983) *J. Neurosci.* **3**, 506–516.
6. Kettenmann, H. & Ransom, B. R. (1988) *Glia* **1**, 64–73.
7. Fischer, G. & Kettenmann, H. (1985) *Exp. Cell Res.* **159**, 273–279.
8. Butt, A. M. & Ransom, B. R. (1989) *Glia* **2**, 470–475.
9. Anders, J. J. (1988) *Glia* **1**, 371–379.
10. Raff, M. C. (1989) *Science* **243**, 1450–1455.
11. Raff, M. C., Abney, E. R., Cohen, J., Lindsay, R. & Noble, M. (1983) *J. Neurosci.* **3**, 1289–1300.
12. Minturn, J. E., Black, J. A., Angelides, K. J. & Waxman, S. G. (1990) *Glia* **3**, 358–367.
13. Barres, B. A., Chun, L. L. Y. & Corey, D. P. (1990) *Annu. Rev. Neurosci.* **13**, 441–474.
14. Levi, G., Gallo, V. & Ciotti, M. T. (1986) *Proc. Natl. Acad. Sci. USA* **83**, 1504–1508.
15. Sontheimer, H., Ransom, B. R., Cornell-Bell, A H., Black, J. A. & Waxman, S. G. (1990) *J. Neurophysiol.*, in press.
16. Hamill, O. P., Marty, A., Neher, E., Sakmann, B. & Sigworth, F. J. (1981) *Pflügers Arch.* **391**, 85–100.
17. Spray, D. C., Saez, J. C., Brosius, D., Bennett, M. V. L. & Hertzberg, E. L. (1986) *Proc. Natl. Acad. Sci. USA* **83**, 5494–5497.
18. Somogyi, R. & Kolb, H. A. (1988) *Eur. J. Physiol.* **412**, 54–65.
19. Sontheimer, H., Minturn, J. E., Ransom, B. R., Black, J. A., Cornell-Bell, A. H. & Waxman, S. G. (1990) *Ann. N.Y. Acad. Sci.*, in press.
20. Barres, B. A., Chun, L. L. Y. & Corey, D. P. (1989) *Neuron* **2**, 1375–1388.
21. Minturn, J. E., Sontheimer, H., Black, J. A., Angelides, K. J., Ransom, B. R., Ritchie, J. M. & Waxman, S. G. (1990) *Ann. N.Y. Acad. Sci.*, in press.
22. Murphey, A. D., Hadley, R. D. & Kater, S. B. (1983) *J. Neurosci.* **3**, 1422–1429.
23. Mobbs, P., Brew, H. & Attwell, D. (1988) *Brain Res.* **460**, 235–245.
24. Ransom, B. R. & Kettenmann, H. (1990) *Glia* **3**, 258–266.
25. Bennett, M. V. L. (1966) *Ann. N.Y. Acad. Sci.* **137**, 509–539.
26. Spray, D. C. & Bennett, M. V. L. (1985) *Annu. Rev. Physiol.* **47**, 281–303.
27. Orkand, R. K. (1977) in *Handbook of Physiology*, eds. Brookhart, J. & Mountcastle, V. (Am. Physiol. Soc., Bethesda, MD), Vol. 1, pp. 855–875.
28. Gardner-Medwin, A. R. (1985) *J. Physiol. (London)* **365**, 52P.
29. Newman, E. A. (1984) *Nature (London)* **309**, 155–157.
30. Conner, J. D., Detwiler, P. B. & Sarthy, P. V. (1985) *J. Physiol. (London)* **362**, 79–82.
31. Miller, H. R., Fulton, B. P. & Raff, M. C. (1989) *Eur. J. Neurosci.* **1**, 172–180.
32. Waxman, S. G. & Black, J. A. (1984) *Brain Res.* **308**, 77–78.